- a constant optical depth, $\tau_\lambda = \bar{\chi}_\lambda \langle L \rangle$, across the beam cross section (so that the absorption is independent of the point of origin of a beam element emitted from the source)

- atomic absoption cross sections that depend only upon the atomic physics, i.e., are independent of the local physical environment [under certain conditions $\alpha(\lambda)$ can be modified, such as in the presence of magnetic fields or high gas pressure]

- an isothermal absorbing gas cloud, so that the total absorption cross section, $\sigma(\lambda)$, is independent of line of sight location through the cloud [allowing $\sigma(\lambda)$ to be factored out of optical depth integral (Eq. 5.30)]

As each of these assumptions is relaxed, either the solution to the radiative transfer and/or the expression for the optical depth become progressively more complex. Eq. 5.31 is employed for most all applications in the astronomical literature.

In practice, greater complexity is applied when the structure of a global absorbing phenomenon is being studied or the kinematics of such a structure is being studied. Examples of applications for which the models of the radiative transfer and/or optical depth are more complex include intergalactic gas structures undergoing cosmological expansion (e.g., Gunn & Peterson, 1965), rotating galactic halos with density gradients (e.g., Weisheit, 1978), infalling clouds into galactic halos and rotating galaxy disk kinematics (e.g., Lanzetta & Bowen, 1992) and outflowing winds associated with the background source itself (e.g., Vilkovoiskij & Irwin, 2001).

The reader is also refered to the books on stellar atmospheres by Mihalas (1978) and by Gray (1992). These authors, especially Mihalas, develop formalism of the optical depth for absorption models that incorporate systematic gas dynamics.

5.6 Spectrophotometry and Magnitudes

In certain applications, it may be of interest to measure the observed flux, F_λ, summed over a desired wavelength range. This converts the energy collected per unit area per unit time per unit wavelength to energy collected per unit area per unit time. The flux per unit wavelength, F_λ is sometimes referred to as the flux density, whereas the quantity $F(\lambda) = \lambda F_\lambda$ is referred to as the flux (in this text, this distinction of nomenclature is applied only when the context of discussion requires it; the subscript always implies flux density). The flux density over a selected wavelength range is written

$$F_\lambda = \int_{\lambda_-}^{\lambda_+} F_\lambda \, d\lambda, \tag{5.32}$$

where λ_- and λ_+ are the lower and upper limits of the wavelength range.

Alternatively, the flux density and flux can be measured or converted to frequency units, where $F(\nu) = \nu F_\nu$, where the frequency flux density, F_ν, has units of [erg s^{-1} cm^{-2} Hz^{-1}]. The relationship between F_ν and F_λ derive from energy conservation and the relationship $c = \nu\lambda$. We have

$$F_\lambda d\lambda = F_\nu d\nu, \qquad F_\lambda = \frac{c}{\lambda^2} F_\nu \,. \tag{5.33}$$

In the application of Eq. 5.33, to preserve units between F_λ and F_ν, the factor $d\nu/d\lambda = c/\lambda^2$ is computed in "mixed" units. Writing $d\nu/d\lambda = (c/\lambda)/\lambda$, we compute c/λ in cgs units with the final λ in [angströms].

In imaging, it is common that the observed flux is measured using a fixed filtered band pass. It is also common practice that the filter is a member of a predetermined suite of filters comprising a photometric system (see below). These photometric systems are calibrated using the magnitude system. Magnitudes are unitless numbers on an inverted logarithmic scale that are based upon flux ratios. The zero points are defined by the fluxes of standard objects accounting for the filter band–pass response of the filters.

In cases where spectroscopic data are in hand but the magnitude of the source is desired in a certain band pass, one can perform spectrophotometry. If the response function of the filter with band pass y is $R_y(\lambda)$ over the wavelength range λ_{y^-} to λ_{y^+}, then the measured band pass flux (modulated by the filter band pass) is

$$F_y = \int_{\lambda_{y^-}}^{\lambda_{y^+}} R_y(\lambda)\, F_\lambda \, d\lambda \,. \tag{5.34}$$

The response functions are the probability of transmission at each wavelength and obey

$$\int_{\lambda_{y^-}}^{\lambda_{y^+}} R_y(\lambda)\, d\lambda = 1, \tag{5.35}$$

where the integration is take over a broad enough wavelength range such that the filter response vanishes, i.e., $R_y(\lambda) = 0$ for $\lambda = \lambda_{y^-}$ and $\lambda = \lambda_{y^+}$.

5.6.1 Apparent magnitude

The flux density measured on the magnitude scale is defined by

$$m_\lambda = -2.5 \log F_\lambda \qquad m_\nu = -2.5 \log F_\nu \tag{5.36}$$

As such, magnitudes provide an alternative scale with which flux densities can be quoted. It is not uncommon to see the flux densities of stars and other sources presented in m_λ or m_ν.

The band–pass apparent magnitude is defined using the ratio of the band–pass flux (Eq, 5.34) of the object to that of a standard source. In a band pass y,

$$m_y = -2.5 \log \left\{ \frac{F_y}{F_y^s} \right\} \tag{5.37}$$

where F_y is the band pass y flux of the object and F_y^s is band pass y flux of the standard source. Note that if the object band pass flux equals the source band pass flux, i.e., $F_y = F_y^s$, then $m_y = 0$. Thus, the standard source provides the zero point of the apparent magnitude scale. Also, note that m_y decreases as the ratio F_y/F_y^s increases. Objects with $F_y > F_y^s$ have $m_y < 0$ and those with $F_y > F_y^s$ have $m_y > 0$.

Flux ratios

Apparent magnitudes provide a simple relationship in which the ratio of the band pass fluxes of two distinct objects can be determined by the difference of their apparent magnitudes. Through the definition of magnitudes (Eq. 5.37), we have

$$m_y^{(1)} - m_y^{(2)} = -2.5 \log \left\{ \frac{F_y^{(1)}}{F_y^s} \right\} + 2.5 \log \left\{ \frac{F_y^{(2)}}{F_y^s} \right\} = -2.5 \log \left\{ \frac{F_y^{(1)}}{F_y^{(2)}} \right\}, \quad (5.38)$$

which can be inverted to obtain,

$$\frac{F_y^{(1)}}{F_y^{(2)}} = 10^{-0.4\left[m_y^{(1)} - m_y^{(2)}\right]}. \quad (5.39)$$

Note that every integer difference in the magnitudes of two objects corresponds to a factor of $10^{-0.4} = 2.5$ in their flux ratios. The term "dex" is often used; it is shorthand for "decade" on the logarithmic scale. For instance, the flux ratio of ± 2.5 corresponds to ∓ 0.4 [dex] on the magnitude scale.

5.6.2 Photometric systems

There are two main photometric systems employed in the astronomical sciences, the Vega system and the AB system. There are a plethora of filter suites, including the Johnson–Cousins, Washington, Gunn, Sloan Digital Sky Survey, Hipparcos–Tycho, and *Hubble Space Telescope* WFPC–2 and 3, and ACIS sets. For a general review see Bessell (2005). For brevity, we employ the Johnson–Cousin $UBVRI$ system for purposes of illustration. The $UVBRI$ filter response functions (renormalized to a peak transmission of unity) are illustrated in Figure 5.7. For example, the $y = V$ ("visual" band) filter has an effective central wavelength of 5500 Å with a band pass ranging from 4700–7400 Å.

Vega system

The Vega system is calibrated using the flux density of the A0 V star Vega (or sometimes the mean of a sample of unreddenned A0 V Pop I stars). The flux density of Vega (Oke, 1990)[1] is presented in Figure 5.7 as the thin solid

[1]The electronic data were obtained from the on–line archive of optical and UV spectrophotmetric flux standard stars made available by the European Southern Observatory. (*http://www.eso.org/sci/observing/tools/standards/spectra/*)

curve (with absorption features). Because A0 V stars do not have a flat flux density, the calibration band pass flux, $F_y^{(\mathrm{Vega})}$ is different for each band pass. For additional information see Oke & Gunn (1983); Bessell (1990). For information on the Sloan filter suite and calibration, see Smith *et al.* (2002).

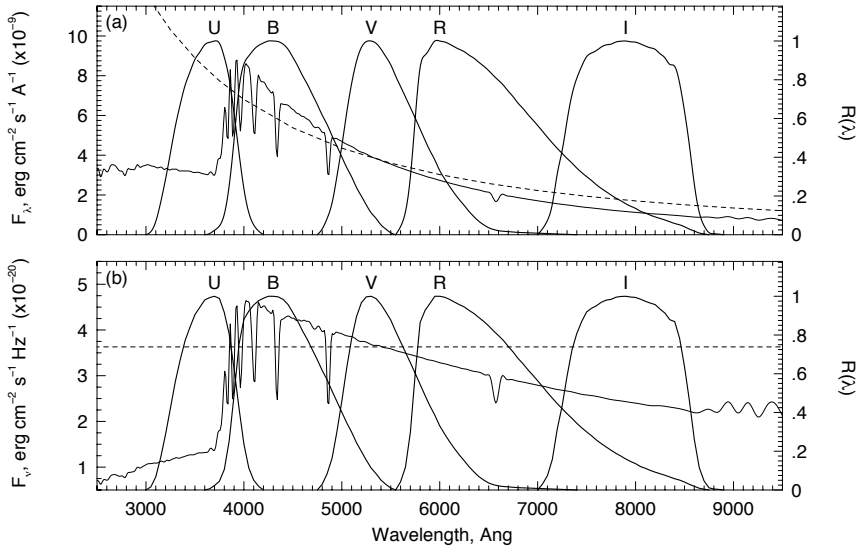

Figure 5.7: (*a*) The flux densities, F_λ, of Vega (thin solid curve) and the hypothetical AB source (dashed curve). (*b*) The flux densities, F_ν, of Vega (thin solid curve) and the hypothetical AB source (dashed curve). Superimposed are the Johnson–Cousins $UBVRI$ filter response curves normalized to unity at their peak transmissions. The differences between the calibration magnitude of Vega and that of the AB magnitude are listed in Table 5.1.

AB system

For AB magnitudes, there is no physical standard source, but simply a definition of a hypothetical source with $F_\nu^{(\mathrm{AB})} = 3.63 \times 10^{-20}$ [erg s^{-1} cm^{-2} Hz^{-1}] for all ν (a flat frequency flux density distribution). This is not a flat flux density in wavelength, $F_\lambda^{(\mathrm{AB})} = 0.1092/\lambda^2$ [erg s^{-1} cm^{-2} Å^{-1}] (where λ is [angströms]). The AB flux density is presented in Figure 5.7 as the thin dashed curve.

Because F_ν is a constant, and the filter responses have unity normalization (Eq. 5.35), we have $F_y^{(\mathrm{AB})} = F_\nu^{(\mathrm{AB})}$, yielding $-2.5\log\{3.63\times10^{-20}\} = 48.60$. Thus, from the definition of apparent magnitude (Eq. 5.37),

$$m_y(\mathrm{AB}) = -2.5\log F_y - 48.60 = -2.5\log F_\nu - 48.60 = m_\nu - 48.60 \qquad (5.40)$$

for all band passes, where m_ν is the magnitude of the flux density as defined in Eq. 5.36. Note that Eq. 5.40 (and the constant -48.60) applies only if the band pass flux is determined using frequency units. As such, AB magnitudes in frequncy units are equivalent to the flux density magnitude, m_ν, scaled to the hypothetical AB source.

Contrasting systems

In Figure 5.7*a*, the standard Vega and AB flux density distributions, $F_\lambda^{(\mathrm{Vega})}$ and $F_\lambda^{(\mathrm{AB})}$, are shown. In Figure 5.7*b*, $F_\nu^{(\mathrm{Vega})}$ and $F_\lambda^{(\mathrm{AB})}$ are shown. The Johnson–Cousins $UVBRI$ band pass response curves[2] are superimposed (thick solid curves). Vega is shown as the thin solid curve (which exhibits aborption features), and the AB source is shown as the smooth dashed curve. The definition of the AB standard "source" flux density was chosen to give $m_V(\mathrm{AB}) = m_V$, or more precisely

$$\int_{4700}^{7400} R_V(\lambda)\, F_\lambda^{(\mathrm{Vega})}\, d\lambda = \int_{4700}^{7400} R_V(\lambda)\, F_\lambda^{(\mathrm{AB})}\, d\lambda\,, \tag{5.41}$$

(or the equivalent integrals over frequency). However, the latest calibration of Vega yields a difference of 0.044 magnitudes. Note that the flux density curves are normalized (by definition for AB magnitudes) near the center of the response curve for the V filter.

In Table 5.1, the central (effective) wavelength, λ_y, and the band pass width, $\Delta\lambda_y/\lambda_y$, are listed for the Johnson–Cousins $UBVRI$ filter suite. Also listed are the values of $F_\nu^{(\mathrm{Vega})}$ [erg s^{-1} cm^{-2} Hz^{-1}] at ν_y and $F_\lambda^{(\mathrm{Vega})}$ [erg s^{-1} cm^{-2} Å^{-1}] at λ_y. The values of the latter can be visually confirmed by inspection of Figure 5.7. The last column lists the magnitude difference between the Johnson–Cousins Vega system and the Johnson–Cousins AB system, $m_y - m_y(\mathrm{AB}) = \Delta m_y$, i.e., the quantity added to the Johnson magnitude in band pass y to obtain the AB magnitude in that band pass.

Table 5.1: Vega and AB Magnitude Data

Band pass (y)	λ_y [Å]	$\Delta\lambda_y/\lambda_y$	$F_\nu^{(\mathrm{Vega})}$ [10^{-20}]	$F_\lambda^{(\mathrm{Vega})}$ [10^{-9}]	Δm_y
U	3600	0.15	1.81	3.18	$\cdots$
B	4400	0.22	4.26	6.60	-0.163
V	5500	0.16	3.64	3.61	-0.044
R	6400	0.23	3.08	2.26	$+0.055$
I	7900	0.19	2.55	1.23	$+0.309$

In imaging studies, one measures F_y directly. In spectroscopic studies, F_y must be computed using Eq. 5.34 from the measured F_λ or F_ν. In practice, imaging studies are almost always more accurate because accurately measuring the flux spectroscopically is complicated by additional wavelength effects. In particular, one must be sure that all the light from the object passes through

[2]Electronic data from *ftp://ftp.noao.edu/kpno/filters/4Inch_List.html* .

the slit (if the slit is narrower than the seeing disk of the object, then some light will be lost at the slit).

5.6.3 Absolute magnitude and luminosity

The absolute magnitude in band pass y, M_y, is defined as the apparent magnitude that an observer would measure at a distance of $D = 10$ [pc] from the source. Whereas apparent magnitude differences relate band pass flux ratios, absolute magnitude differences relate band pass luminosity ratios. Thus, in a sense, M_y is a surrogate for band–pass luminosity through the normalization of the band–pass flux to a standardized distance. To account for the finite band pass, the luminosity density, L_λ, is employed,

$$L(\lambda) = \lambda L_\lambda, \tag{5.42}$$

where $L(\lambda)$ is in [units erg s^{-1}], and L_λ is in units [erg s^{-1} Å^{-1}]. The coversion from L_λ to L_ν follows the relations for the flux density as given in Eq. 5.33. The integrated luminosity density in the band pass is

$$L_y = \int_{\lambda_{y^-}}^{\lambda_{y^+}} R_y(\lambda) L_\lambda \, d\lambda \,. \tag{5.43}$$

The relationship between the flux density and the luminosity density is

$$F_\lambda = \frac{L_\lambda}{4\pi D^2}. \tag{5.44}$$

From Eqs. 5.34, 5.37 and 5.44, the apparent magnitude of an object observed in band pass y can be written in terms of luminosity

$$m_y = -2.5 \log \left\{ \int_{\lambda_{y^-}}^{\lambda_{y^+}} R_y(\lambda) \frac{L_\lambda}{4\pi D^2} \, d\lambda \right\} + 2.5 \log F_y^s. \tag{5.45}$$

By definition, the absolute magnitude is obtained by setting $D = 10$ [pc],

$$M_y = -2.5 \log \left\{ \int_{\lambda_{y^-}}^{\lambda_{y^+}} R_y(\lambda) \frac{L_\lambda}{4\pi (10 \text{ pc})^2} \, d\lambda \right\} + 2.5 \log F_y^s, \tag{5.46}$$

The difference of the above two equations, $m_y - M_y$, is called the distance modulus, denoted DM,

$$\text{DM} = 5 \log \left\{ \frac{D}{10 \text{ pc}} \right\} = 5 \log D - 5, \tag{5.47}$$

where the distance to the object, D, is expressed in [parsecs]. Thus, if the apparent magnitude and distance to an object is measured, the absolute magnitude can be computed from

$$M_y = m_y - \text{DM}, \tag{5.48}$$

Often, for a population of object (such as galaxies, etc.), there is a measured characteristic absolute magnitude, M_y^*, for the band pass, which, according to Eq. 5.46, corresponds to a characterstic luminosity for the band pass, L_y^*. This characteristic luminosity might be, for example, the average band pass luminosity for a population of object. Through the definition of magnitudes (Eqs. 5.37 and 5.46), and applying steps analagous to those obtained to derive Eq. 5.38, we have

$$M_y - M_y^* = -2.5 \log \left\{ \frac{L_y}{L_y^*} \right\}, \tag{5.49}$$

which can be inverted to obtain the ratio of the luminosity of the object to the characteristic luminosity of the population,

$$\frac{L_y}{L_y^*} = 10^{-0.4\left[M_y - M_y^*\right]}. \tag{5.50}$$

5.6.4 Cosmological Sources

The above treatment of the apparent and absolute magnitudes presupposes that the source object is in the same cosmological reference frame as the observer. Cosmological objects can have substantially redshifted spectral energy distributions, such that the flux density observed in band pass y at the observer does not correspond to the same band pass in the frame of the source. The cosmological effects altering the observed flux density of a redshifted source are discussed in Chapter 14. These effects require that a corrective term be applied to the band pass flux integrals in order to deduce the apparent and absolute magnitude in the rest frame of the object. These corrections, called K–corrections, are discussed in § 14.7.

5.7 Atmospheric attenuated flux

The quantity F_λ is the observed flux incident upon the upper atmosphere of Earth. Before this flux is recorded for subsequent analysis, the beam first suffers wavelength dependent attenuation while passing through the atmosphere. We quantify the atmospheric transmission at wavelength λ as $\epsilon_\lambda^{\rm A}$, which equals the ratio of the flux entering the telescope to the observed flux entering the upper atmosphere, F_λ. The form of $\epsilon_\lambda^{\rm A}$ can be complex and include atmospheric absorption lines and bands, which are commonly known as telluric features. Furthermore, the magnitude of $\epsilon_\lambda^{\rm A}$ is proportional to the path length through the atmosphere.

Defining atmospheric attenuated flux as $F_\lambda^{\rm A}$,

$$\epsilon_\lambda^{\rm A} = \frac{F_\lambda^{\rm A}}{F_\lambda} = \exp\{-\tau_\lambda^{\rm A}\}, \tag{5.51}$$

where $\tau_\lambda^{\rm A}$ is the optical depth of the atmosphere. The optical depth increases with the zenith angle, denoted z, which is the angle of the line of sight to the

source measured from the local zenith of the telescope. For a constant density plane parallel model of the atmosphere,

$$\tau_\lambda^{\rm A}(z) = \tau_\lambda^{\rm A}(0)\sec z, \tag{5.52}$$

where $\tau_\lambda^{\rm A}(0)$ is the atmospheric optical depth at the zenith ($z = 0$). A commonly used term to quantify the attentuation through the atmosphere is the "airmass", defined as the ratio of the optical depth toward the zenith to the optical depth at zenith angle z,

$$\text{airmass} = \frac{\tau_\lambda^{\rm A}(z)}{\tau_\lambda^{\rm A}(0)} = \sec z. \tag{5.53}$$

Note that the $\sec z$ dependence applies only under the assumption of a constant density plane parallel atmosphere; it applies well for small z. Higher accuracy approximations can be found in Kasten & Young (1989). Technically, airmass of unity is defined at sea level, but it is common that this normalization is not included in the definition so that airmass is measured with respect to the local elevation of the telescope facility. Thus, the zenith sightline is referred to as "unit airmass". In the most general form, we have

$$\epsilon_\lambda^{\rm A}(z) = \exp\{-\tau_\lambda^{\rm A}(z)\}\,. \tag{5.54}$$

Thus, the flux entering the telescope at angle z from the zenith, which we call the "attenuated flux", is then given by

$$\tilde{F}_\lambda^{\rm A} = \epsilon_\lambda^{\rm A}(z)\,F_\lambda = \epsilon_\lambda^{\rm A}(z)\frac{R^2}{D^2}\,\mathcal{F}_\lambda \exp\{-\tau_\lambda\} = \tilde{F}_\lambda^{\rm A_0}\exp\{-\tau_\lambda\}\,, \tag{5.55}$$

where τ_λ is the optical depth of an absorption feature in the observed flux spectrum and the "attenuated continuum flux" (the attenuated flux in the absence of an intervening absorbing cloud ($\tau_\lambda = 0$) is

$$\tilde{F}_\lambda^{\rm A_0} = \epsilon_\lambda^{\rm A}(z)\frac{R^2}{D^2}\mathcal{F}_\lambda = \epsilon_\lambda^{\rm A}(z)\frac{R^2}{D^2}\,\pi\,\mathcal{I}_\lambda. \tag{5.56}$$

As we will discuss in detail in Chapter 6, further modification to the final recorded flux occurs as the light interacts with the optical elements of the telescope and the spectrograph before the light beam impinges upon the recording apparatus, i.e., the detector. Fortunately, all these attenuations and modifications are multiplicative, so that one can recover the observed flux, F_λ, via a process known as flux calibration (see Chapter 7).

References

Bessell, M. S. 1990, UBVRI passbands, Pub. Astron. Soc. Pac., **102**, 1181

Bessell, M. S. 2005, Standard photometric systems, *Ann. Rev. Astron. & Astroph.*, **43**, 293

Gray, D. F. 1992, *The Observational and Analysis of Stellar Photospheres*, Cambridge University Press

Gunn, J. E., & Peterson, B. A. 1965, On the density of neutral hydrogen in intergalactic space, *Ap. J.*, **142**, 1633

Kasten, F., & Young A. T. 1989, Revised optical air mass tables and approximation formula, *Applied Optics*, **28**, issue 22, 4734

Lanzetta, K., & Bowen, D. V. 1992, The kinematics of intermeidate–redshift gaseous galaxy halos, *Ap. J.*, **391**, 48

Mihalas, D. 1978, *Stellar Atmospheres*, W. H. Freeman & Company

Oke, J. B., & Gunn, J. E. 1983, "Secondary Standard Stars for Absolute Spectrophotometry," *Ap. J.*, **266**, 713

Oke, J. B. 1990, Faint spectrophotometric standard stars, *A. J.*, **99**, 1621

Smith, J. A., *et al.* 2002, "The u'g'r'i'z' standard–star system," *A. J.*, **123**, 2121

Weisheit, J. C. 1978, On the use of line shapes in the analysis of QSO absorption spectra, *Ap. J.*, **219**, 829

Vilkoviskij, Y, & Irwin, M. J. 2002, The spectrum of BAL Q1303+308: intrinisc variability and line locking stability, *M.N.R.A.S.*, **321**, 1